Vol. 211, No. 1, 1995 BIOCHEMICAL AND BIOPHYSICAL RESEARCH COMMUNICATIONS
June 6, 1995 Pages 219-225

Direct measurement for elasticity of myosin head

Hitoshi Suda*, Masaya Sugimoto, Masafumi Chiba† and Chikao Uemura†

Departments of Biological Science and Technology and †Materials and Technology,
Tokai University, 317 Nishino, Numazu, Shizuoka 410-03, Japan

Received April 22, 1995

SUMMARY: During muscle contraction, chemical energy from ATP hydrolysis is converted to the relative sliding movement of actin and myosin filaments. In order to elucidate the molecular mechanism of sliding-force generation, it is a crucial clue to know an elastic modulus of myosin. Here, we report direct measurements of Young's modulus of myosin head (myosin subfragment-1) isolated from rabbit skeletal muscle, using a surface forces apparatus. Our results show that the elasticity of myosin subfragment-1 has direction and is about 0.3 GPa along the long axis during ATP hydrolysis. When the bow-shaped subfragment-1 is modelled as an elastic rod, the stiffness and the bending fluctuations of subfragment-1 are calculated to be 3 ~ 7 pN/nm and about 1 nm, respectively. These results strongly support a model of multiple power strokes rather than the conventional tilting-crossbridge model.

Muscle contraction occurs as a result of the transduction of chemical energy into mechanical energy. Myosin generates sliding forces with ATP hydrolysis by interacting with an actin filament. Although the actomyosin system has been extensively studied, the coupling mechanism of mechanochemical energy transduction remains unclear. The conventional crossbridge model (1-4) of muscle contraction postulates that the heads of the myosin molecules (the crossbridges) projecting from the thick filaments, for each ATP hydrolysis, attach to actin in the thin filaments and undergoes a conformational change or one power stroke before subsequently detaching, pull the thin filaments toward the center of the sarcomere, and detach. The force or filament sliding movement might be generated by tilting the attached myosin head. This theory assumes that the myosin step size, or movement of actin relative to myosin for each ATP hydrolysis, is less than 40 nm, a value limited by the physical dimensions of the crossbridge (2). On the other hand, by *in vitro* movement assays, it has been found that myosin subfragment-1 (S1) is sufficient to move actin filament (5). Therefore, if the conventional crossbridge theory is correct and the sliding force is generated by swinging motion of S1, it suggests that the origin of force production resides in the stiffness or elasticity of S1. In the present stage, as a direct evidence, to directly measure the elasticity of S1 is an important key point for the molecular mechanism of muscle contraction. To address this problem, we tried the direct measurement for the elasticity of S1 *in vitro* by using the surface forces apparatus (SFA) (6). Through the mechanical properties obtained for S1 in an active state, in this paper, we discuss whether or not our results are consistent with the predictions

*To whom correspondence should be addressed. Fax: 81-559-68-1156. E-mail: suda@fb.u-tokai.ac.jp.

0006-291X/95 $5.00

from the conventional tilting-crossbridge models based on the conformational change of myosin head, specially the analytical A.F.Huxley's model.

Materials and Methods

Myosin was prepared from rabbit back and leg muscles. Myosin subfragment-1 was prepared by chymotryptic digestion of myosin according to the method of Weeds & Pope (7), and it was purified by Sephacryl S-300. The S1 concentration was determined spectrometrically by taking absorption coefficient of A_{280nm}= 0.75 $(mg/ml)^{-1}cm^{-1}$. Before using the S1 solution at experiment, it was centrifuged at about 150,000 g for 6 hours. The concentration of S1 solution was adjusted to 0.1 ~ 0.2 mg/ml. All chemicals used were of analytical grade. All water used was purified by doubly distilling ultra pure water (≥ 18 MΩ•cm) in an all-Pyrex still. The dust in solution was removed by Molcat-L (MILLIPORE; LCC, NMWL5000). The mica used was best quality muscovite ruby mica (Hakuto Co., Tokyo). The surface forces between two molecularly smooth curved (R ≈ 1 cm) mica surfaces as a function of D were measured using the method developed by Israelachvili and Adams (6). As a SFA, Mark IV (ANUTECH Pty Ltd.) was employed. Two mica surfaces were glued with an epoxy resin (EPEKOTE 1004, NISSHIN EM Co., Ltd.) onto half cylindrical silica discs and mounted in a crossed cylinder configuration. The measured F divided by R is related to the free energy of interaction per unit area, G, between two flat surfaces according to the Derjaguin approximation (8), $F(D)/R = 2\pi G(D)$. The distance between the mica surfaces was determined with an accuracy of about 0.1 nm using multiple beam interferometry, and the refractive index of the intervening medium was measured. The interaction force was determined from the deflection of a double cantilever spring (spring constant ≈ 140 N/m) supporting the lower surface and the normalized force F/R was determined down to 10 μN/m. All preparing operations were performed in a laminar flow cabinet under essentially dust-free conditions. The mica-mica contact position was first measured and then the surfaces were separated by about several millimeters apart at which the chamber was emptied. The S1 droplet of a volume of 50 ~ 100 μl was mounted upon the lower mica surface, and S1 molecules in solution were adsorbed onto the mica during 10 ~ 30 min. Then the ATP or ATP-free solution (~ 35 ml) was injected into the teflon bath (volume ≈ 35 cm^3), where the exchange method of solution was improved as shown in Fig. 1 and it was essential to this study. The refractive-index increment of S1 solution was 0.2275 ml/gr at 25°C, using an Abbe refractometer (Shimazu Seisakusho, Ltd.; Bausch&Lomb type). The estimated error in determining the adsorbed layer thickness is ± 0.3 nm. All experiments were carried out at 25 ± 0.2°C.

Results and Discussion

Fig. 2 *A* and *B* show a logarithmic plot of the surface forces F normalized by the local mean radius R, F/R, against the surface separation D between one bare mica surface and the other surface coated by S1 molecules onto mica, in the presence and absence of ATP. Surface forces were measured as a function of distance in inward approach, using an improved SFA. All the data presented in this paper are relative to the contact position of the mica sheets in ultra-pure dry nitrogen, i.e., at D=0, where the two mica surfaces are in molecular contact. It is important to know the position of the adsorbed protein surface. The repulsive forces commenced at surface separations of 40 ~ 50 nm, and increased exponentially with distance until the surfaces were about 17.0 nm in the presence of ATP (case *A*) and 10.0 nm in the absence of ATP (case *B*) from the mica contact, where these values are defined as a critical distance Dc. Further compression of the surfaces resulted in steeply rising repulsive forces, with decreasing the surface separation. Because of strong short-range repulsive forces, the mica surfaces were prevented from coming into molecular mica-mica contact. The origin of this strong short-range repulsion is due to steric interactions of the S1 molecules between two mica surfaces. At the Dc, the refractive index was

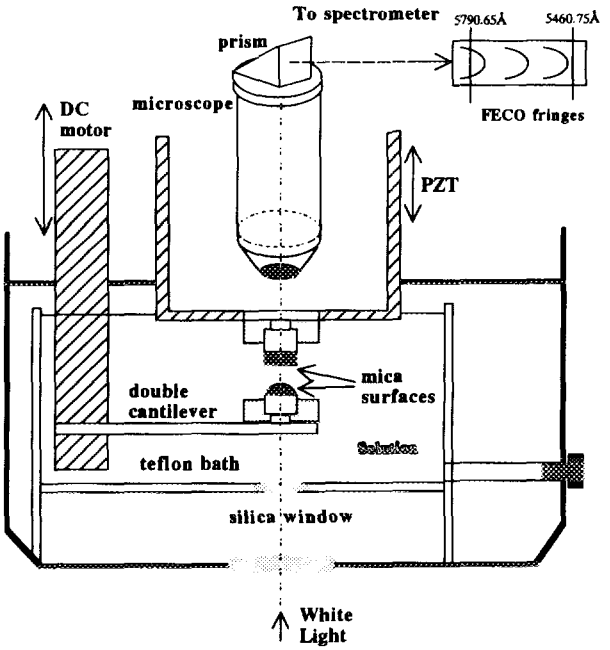

Fig. 1. Schematic diagram of the improved SFA which has an exchangeable system of solution.

1.410 in *A* and 1.475 in *B*. Taking account of the refractive-increment against S1 concentration, the adsorbed density (9) of S1 for A and B was calculated to be 5.36 mg/m^2 and 6.18 mg/m^2, respectively. Thus the occupied area per S1 (M.W. = 11,5000) for *A* and *B* was evaluated as (5.6

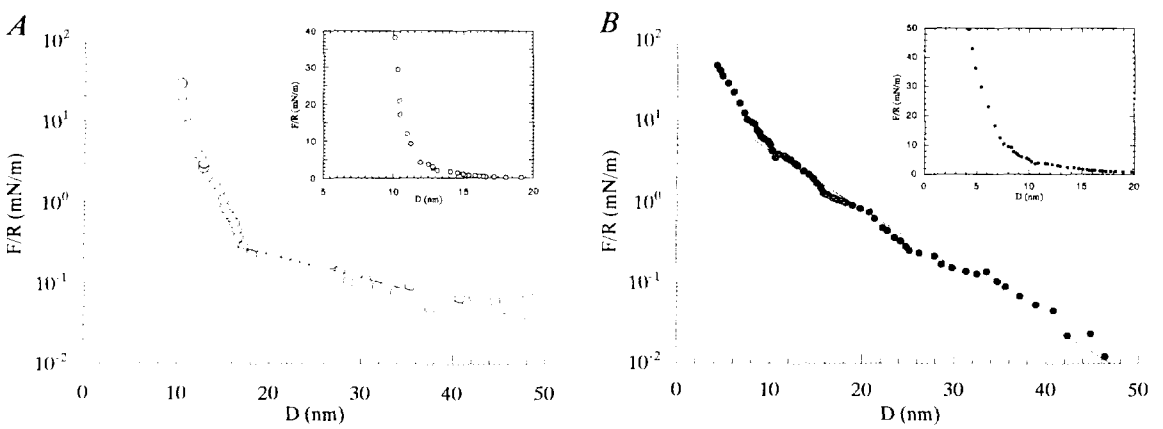

Fig. 2. The normalized forces F/R as a function of surface separation D between one S1-coated surface and one bare mica surface. Surface forces were measured on approach in two different solutions; *A* (o) in an ATP solution (1 mM ATP, 15 mM KCl, 4 mM $MgCl_2$, 5 mM Tris-Maleic Acid, pH 8.0) and, *B* (•) in an ATP-free solution (15 mM KCl, 4 mM $MgCl_2$, 5 mM Tris-Maleic Acid, pH 8.0). The solid line is the fit of the data at the long range to an exponential function; *A*, F/R (mN/m) = 0.6734 exp(- 0.05617 D) and *B*, F/R (mN/m) = 17.196 exp(- 0.15242 D). The insets show the normalized forces plotted on a linear scale.

nm)^2 and (5.2 nm)^2, respectively. It seems likely that adsorbed S1 molecules are closely packing. The apparent Debye screening length in the ATP-containing and ATP-free solution were 1.1 ± 0.3 nm (mean ± s.d., n=5) and 1.3 ± 0.2 nm (n=5) in between two bare mica surfaces, respectively, whereas 11.3 ± 6.5 nm (n=8) and 8.0 ± 4.3 nm (n=13) in the S1-coated system, respectively. The results were not expected by the classical DLVO theory (10&11) as in the SFA-measurement of ribonuclease A (12). One possibility can be attributed to a diffuseness of the outer Helmholtz plane resulting from surface heterogeneity (13). Since the ATPase activity of S1 adsorbed onto mica is recognized by using *in vitro* motility assay (Y.Y.Toyoshima, personal communication), the protein denaturation may be excluded presumably. Further investigation into the origin of the long-range repulsive effect must be pursued.

As the distance became shorter than Dc, further strong short-range repulsive forces occurred as seen in Fig. 2. At the short range, the force-distance profile deviates drastically from the exponential curve in the long-range that may be due to the repulsive electric double-layer force. During compression of the surfaces, the knee was the point at which the adsorbed S1-layer and the bare mica began to touch and the onset of steep repulsion was observed. Thus the distance at the knee presents a size of S1 on mica. The steric repulsive forces ΔF were purely isolated by subtracting the long-range repulsive forces from the original force profile as shown in Fig. 3. The stress to the S1-layer may be deduced by differentiating ΔF by D. If the linear relation, the Hooke's law, between the strain against the external stress is established, then the slope corresponds to Young's modulus, and the ΔF has to be proportional to the square of the strain by the Derjaguin approximation. Consequently, the proportional coefficient β within Dc - D = 2 nm was determined to be 4.71 x 10^{-3} mN/nm^2 (correlation coeff. r = 0.960) for *A* and 9.78 x 10^{-3}

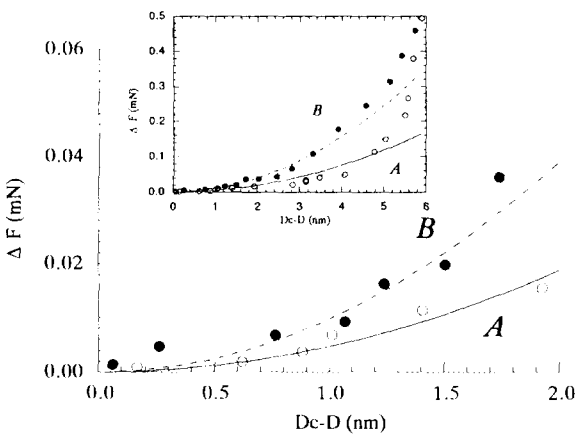

Fig. 3. Steric repulsive forces ΔF as a function of strain (Dc - D). The data in Fig. 2 were analyzed. Experimental points were obtained from the difference between the original force and the exponential force (solid line) in Fig. 2. Here the radii R at *A* and *B* were 1.31 cm and 1.17 cm, respectively. The ΔF curve was fitted by the square of (Dc - D), where Dc indicates the layer thickness of adsorbed S1 that corresponds to the size of molecule. (See text.) The fitting parameter β is related to Young's modulus in the legend of Fig. 4 *a*.

mN/nm^2 (r = 0.978) for *B*. As the fitted curves are extrapolated further from 2 to 6 nm, the deviation from the Hooke's law is clearly observed over 3 ~ 4 nm as shown in the inset of Fig. 3. Here S_0 was 8.23 μm^2 in *A* and 7.35 μm^2 in *B*. If we put those values into the equation of Young's modulus E in the legend of Fig. 4 *a*, Young's moduli for the cases *A* and *B* were derived as 0.34 GPa and 0.26 GPa, respectively. This is the first direct measurement of the elasticity of the myosin head during active hydrolysis of Mg-ATP. If the adsorption amount of S1 was overestimated, the effective contact area would be much smaller, and E would be much larger.

Fig. 4 *a* shows Young's modulus of S1 as a function of the thickness of S1-layer. Those values decreased in the active state from ~ 2 to ~ 0.2 GPa when Dc increased from 4 to 17 nm. The whole feature didn't depend upon the presence nor absence of ATP. Recently, the three-dimensional structure of S1 has revealed that S1 is like a bow or lever-arm with a length of 16.5 nm, a width of 6.5 nm and a thickness of 4.0 nm (14). The Dc = 17.0 nm at the case *A* is almost in agreement with the length of S1. The values of E along the long axis of S1 were 0.34 GPa in the presence of ATP, and 0.88 GPa in the absence of ATP. On the other hand, the average value of E at Dc = 4 ~ 8 nm which corresponds to the dimensions of the width and the thickness is 2.0 GPa. This value is close to that of actin filaments with (~ 3 GPa) and without (~ 2 GPa) tropomyosin

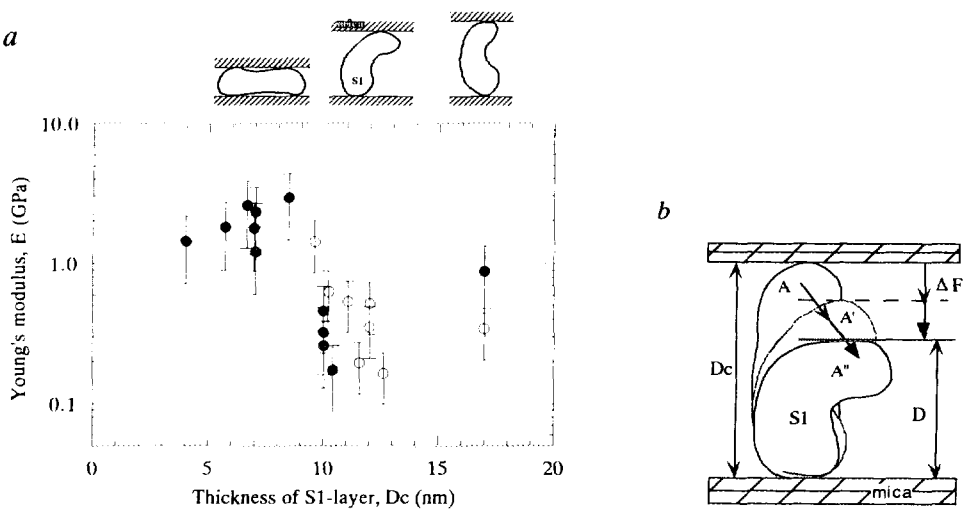

Fig. 4. *a*, Young's modulus E plotted as a function of the adsorbed layer thickness Dc of S1 molecules. Open circle and closed circle indicate the presence and absence of ATP, respectively. According to the Derjaguin approximation, the stress to proteins between two flat surfaces is derived by differentiating F by D between two crossed cylindrical surfaces. Taking account of the Derjaguin approximation and the linear relation of stress-strain that is obeying the Hooke's law, E is given by $2\beta D_c^2/S_0$ as a geometrical problem between two crossed cylindrical surfaces in the SFA system. Here S_0 indicates the contact area, $S_0 = 2\pi Rh$ (R >> D), which is defined by dividing the spherical surface of one bare mica approximately to disks of each step of h = 0.1 nm from the top of the contact point with the other flat protein surface. The error bar means the maximum possible error in the measurement. *b* illustrates the bending deformation (A → A' → A") of the bow-shaped S1 due to the external stress applied between two mica surfaces, at Dc = 17 nm.

(15), microtubles (~ 1 GPa) (16) and other proteins such as myosin subfragment-2 (~ 1 GPa) (17) and collagen (< 9 GPa) (18&19).

When S1 is compressed along the long axis by the external stress, it bends for the sake of the bow-shape as illustrated in Fig. 4 ***b***. When we assume that S1 is a homogeneous elastic rod with a length L and a radius d as a first approximation, the stiffness and the fluctuation displacement of S1 can be calculated by applying the measured elastic modulus in the following equations (20). Also when one end of S1 is fixed and the other end free, the average bending displacement $<\Delta x>$ of the free end due to the force f_b is given by $<\Delta x> = 4f_bL^3/(3\pi d^4E)$, and the mean square of the bending displacement by thermal fluctuation is $<(\Delta x)^2> = 4kTL^3/(3\pi d^4E)$, where k is the Boltzmann constant and T is the absolute temperature. If we put E = 0.2 GPa, L = 17.5 nm, d = 2.5 (or 3.0) nm, f_b = 1 pN and T = 298 K into these equations, we obtain $\sqrt{<(\Delta x)^2>}$ = 1.09 (or 0.76) nm and $<\Delta x>$ = 0.29 (or 0.14) nm in the upper limit. If the size fluctuation of S1 on mica were measured, the expected magnitude would be ~ 1 nm. This value is very close to that of the height fluctuation of active lysozyme which was measured by the atomic force microscope (21). Then, the stiffness of S1 can be given by $f_b/<\Delta x>$, which is calculated to be 3.4 (or 7.1) pN/nm. This is much larger than the stiffness (< 1 pN/nm (22&23)) expected in the crossbridge model, while it is in good agreement with the estimated value (larger than 2.5 pN/nm (24)) by taking into account the extensibility of thin filament (25&26) for the stiffness obtained from physiological experiments. Our stiffness (3 ~ 7 pN/nm) deduces that the bending displacement of S1 would be at most 0.4 ~ 1.6 nm per 3 ~ 5 pN for the force generated by a single crossbridge (27). If the myosin step size is 4 ~ 16 nm as predicted by the conventional crossbridge model (< 17 nm (22)), the value of E should be tenfold smaller than 0.2 GPa. However it is unlikely. If the bending displacement (< 2 nm) is produced as one power stroke during one ATP cycle, these results strongly support the model of multiple power strokes (28-30) rather than the conventional crossbridge models, because the myosin step size is larger than 4 nm at the lowest estimate (14,22,24,27-30). In other words, this means that the displacement < 2 nm per power stroke is not consistent with predictions of A.F.Huxley's model (3&4) in which the force generation and the energy transduction are attributed to the elasticity of myosin and one power stroke per ATP.

Our results suggest that the elementary step size due to bending motin of S1 is < 2 nm under the assumption of one power stroke per ATP, provided that the sliding force is due to the elastic force of S1. Here, we could not obtain the significant result that supports the conventional crossbridge models. As the other possible explanation, the origin of force generation might be expected into local actin motions in the thin filament. But it seems unlikely because the bond energy of actin-actin (31) is much higher than the thermal level. We should rule out the conventional theories based on the conformational changes. Therefore, the present results imply that the force in muscle contraction would be generated in the interface between actin and myosin (32).

Acknowledgments: We thank Dr. M.Miki and C.Kota for their critical reading and help. This work was supported by a Grant-in-Aid for Encouragement of Young Scientists (No.05780486) from the Ministry of Education, Science and Culture of Japan.

References

1.Reedy, M.K., Holmes, K.C. & Tregear, R.T. (1965) *Nature (London)* **207**, 1276-1280.
2.Huxley, H.E. (1969) *Science* **164**,1356-1366.
3.Huxley, A.F. (1957) *Prog.Biophys.biophs.Chem.* **7**, 255-317.
4.Huxley, A.F. (1974) *J. Physiol.* **243**, 1-43.
5.Toyoshima, Y.Y., Kron, S.J., McNally, E.M., Niebling, K.R., Toyoshima, C. & Spudich, J.A. (1987) *Nature (London)* **328**, 536-539.
6.Israelachvili, J.N. & Adams, G.E. (1978) *J.Chem.Soc.Faraday Trans. 1* **74**, 975-1001.
7.Weeds, A.G. & Pope, B. (1977) *J.Mol.Biol.* **111**, 129-157.
8.Derjaguin, B.W. (1934) *Kolloid Z.* **69**, 155-167.
9.de Feijter, J.A., Benjamins, J. & Veer, F.A. (1978) *Biopolymer* **17**, 1759-1772.
10.Derjaguin, B.V. & Landau, L. (1941) *Acta Phys.Chim. URSS* **14**, 633-662.
11.Verwey, E.J.W. & Overbeek, J.T.G. (1948) "Theory of the Stability of Lyophobic Colloids." Elsevier, Amsterdam.
12.Lee, C-S. & Belfort, G. (1989) *Proc.Natl.Acad.Sci.U.S.A.* **86**, 8392-8396.
13.Leckband, D.E., Helm, C.A., Israelachivili, J.N. (1993) *Biochemistry* **32**, 1127-1140.
14.Rayment, I., Rypniewski, W.R., Schmidt-Base, K., Smith, R., Tomchick, D.R., Bennig, M.M., Winkelmann, D.A., Wesenberg, G., Holden, H.M. (1993) *Science* **261**, 50-58.
15.Kojima, H., Ishijima, A. & Yanagida, T.(1994) *Proc.Natl.Acad.Sci.U.S.A.* **91**, 12962-12966.
16.Gittes, F., Mickey, B., Nettleton, J. & Howard, J. (1993) *J.Cell Biol.* **120**, 923-934.
17.Hvidt, S., Nestler, F.H.M., Greaser,M.L. & Ferry,J.D.(1982) *Biochemistry* **21**, 4064-4073.
18.Harley, R., James, D., Miller, A. & White, J.W. (1977) *Nature (London)* **267**, 285-287.
19.Hofmann, H., Voss, T. & Kuhn, K. & Engel, J. (1984) *J.Mol.Biol.* **172**, 325-343.
20.Suezaki, Y. & Go, N. (1976) *Biopolymers* **15**, 2137-2153.
21.Radmacher,M., Fritz, M., Hansma, H.B. & Hansma, P.K. (1994) *Science* **265**, 1577-1579.
22.Goldman,Y.E & Huxley, A.F. (1994) *Biophys.J.* **67**, 2131-2133.
23.Pate, E., White, H. & Cooke, R. (1993) *Proc.Natl.Acad.Sci.U.S.A.* **90**, 2451-2455.
24.Irving, M. (1995) *Nature (London)* **374**, 14-15.
25.Huxley, H.E., Stewart, A., Sosa, H. & Irving, T. (1994) *Biophy.J.* **67**, 2411-2421.
26.Wakabayashi, K. Sugimoto, Y., Tanaka, H., Ueno, Y., Takezawa, Y. & Amemiya, Y. (1994) *Biophy.J.* **67**, 2422-2435.
27.Finer, J.T., Simmons, R.M. & Spudich, J.A. (1994) *Nature (London)* **368**, 113-119.
28.Harada,Y.,Sakurada,K.,Aoki,T.,Thomas,D.D. & Yanagida,T.(1990)*J.Mol.Biol.***216**,49-298.
29.Higuchi, H. & Goldman, Y.E. (1991) *Nature (London)* **352**, 352-354.
30.Lombardi, V., Piazzesi, G. & Linari, M. (1992) *Nature (London)* **355**, 638-641.
31.Kishino, A. & Yanagida, T. (1988) *Nature (London)* **334**, 74-76.
32.Suda, H. & Taylor, T. (1993) *J.Theor.Biol.* **161**, 39-50.